IMPROVED CALIBRATION OF CYGNSS MEASUREMENTS FOR DOWNBURSTS IN THE INTERTROPICAL CONVERGENCE ZONE

Rajeswari Balasubramaniam, Christopher S. Ruf

Climate and Space Dept., University of Michigan, Ann Arbor, MI, USA

ABSTRACT

CYGNSS is a space borne GNSS-R mission that uses the GPS L1 signal which usually has negligible attenuation due to rain. However, under heavy precipitation its effects need to be properly accounted for. In this paper, we characterize the effects of precipitation on the CYGNSS Normalized Bistatic Radar Cross Section (NBRCS) resulting from propagation losses, from rain induced surface roughening, and from increased near-surface wind associated with the presence of rain. Proper accounting for these effects is necessary to accurately retrieve ocean surface wind speed under heavy precipitation and, for example, to resolve the horizontal wind shear present in the rain bands of the ITCZ.

Index Terms—CYGNSS, GNSS-R, calibration, precipitation, ITCZ

1. INTRODUCTION

The Intertropical Convergence Zone is a low pressure belt close to the equator which forms the wet ascending branch of the Hadley cell. It is largely characterized by convective activity and thunderstorms driven by uneven solar heating of the Earth. The ITCZ can act as a catalyst for the process of formation of hurricanes near the equator. It is characterized by wind motion in the vertical direction due to convection and negligible horizontal winds. However, the chain of mesoscale thunderstorms in its rain band produces heavy downbursts that cause strong horizontal wind shear in those regions. It is of interest to the research community to measure the magnitude and shear of such winds. Previous wind scatterometer technologies are limited in their ability to measure these winds for two principle reasons. Firstly, the operating frequencies of current and past polar orbiting scatterometers fail to penetrate into regions characterized by heavy precipitation [1]. Secondly, their re-visit period is very large and can fail to resolve the evolution of such fast evolving phenomena.

The CYclone Global Navigation Satellite System (CYGNSS) is a first of its kind GNSS-R complete orbital mission selected by NASA's earth venture program. CYGNSS works at the all-weather GPS L1 frequency of 1575 MHz to measure the bistatic radar cross section of the surface, from which wind speed is retrieved. L band ocean surface scattering is sensitive to wind speed and the GPS signals are less affected by precipitation. However, the effect of precipitation needs to be carefully accounted under heavy precipitation. The CYGNSS microsatellites carry a passive instrument called the Delay Doppler Mapping Instrument (DDMI). The DDMI resolves the received signals into the Delay and Doppler bins by transforming the observed sea surface into iso-delay lines and iso-doppler regions. This forms a 2D representation called the delay-doppler map (DDM) [2] [3], of the forward scattered signal. Each DDMI outputs 4 DDMs per second which are compressed and sent to the ground resulting in a total of 32 sea-surface measurements produced by the CYGNSS constellation per second. The received DDMs undergo Level-1 calibration (A & B) [4] to produce the Bistatic Radar Cross Section (BRCS), effective scattering areas, and Normalized BRCS (NBRCS, σ_0) which is subsequently used in the retrieval algorithm to extract wind speed information in the glistening zone. The current L1 calibration does not correct for attenuation due to precipitation. To effectively measure winds produced in the rain bands of the ITCZ, the NBRCS needs to be corrected for propagation losses and rain induced surface roughening due to heavy precipitation. Once this is done, the values of NBRCS can be accurately associated with high wind speed caused by downbursts.

This paper is organized as follows. Section II describes the L1 calibration performed by CYGNSS; Section III describes the proposed idea for separating and modelling the two fold effect of heavy precipitation, namely, propagation loss and rain induced surface roughening. Section IV describes the impact of the correction on the CYGNSS measurements and in section V the paper concludes with a discussion of the future work in this direction.

2. LEVEL 1 CALIBRATION IN CYGNSS

Individual bins of a DDM are measured in raw, uncalibrated units referred to as counts. The power in the total signal is the product of all the input signals (scattered GPS signals, thermal emission from the Earth and the receiver) multiplied

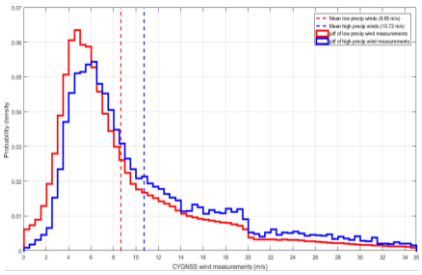

Fig. 1. Probability density function of CYGNSS winds observed at low and high precipitation without correction for path loss or induced roughening due to precipitation.

by the gain of the DDMI receiver and antenna. The Level 1A calibrated DDM represents the received signal power in watts. Level 1B maps DDM of power to DDM of BRCS using the forward model [5]:

$$P_G(\tau,f) = T_i^2 \frac{P_T \lambda^2}{(4\Pi)^3} \iint \frac{G_T(\vec{\rho}) G_R(\vec{\rho}) F(\vec{\rho}) \Lambda^2(\tau,\vec{\rho}) |S(f,\vec{\rho})|^2 \sigma_0(\vec{\rho})}{R_0^2(\vec{\rho}) R^2(\vec{\rho})} d^2\rho \quad (1)$$

Where $P_G(\tau,f)$ is the coherently processed scattered signal power in watts over the coherent integration timeT_i. P_T, λ and G_T are the GPS transmit power, carrier wavelength and antenna gain respectively. R_0 and R are the transmitter to surface and surface to receiver ranges respectively. G_R is the CYGNSS receiver antenna gain and σ_0 is the Normalized Bistatic Radar Cross Section. Λ and S represent the GPS spreading function and the Doppler zone function of the GPS respectively.

The data used in this paper is the Version 2.0 CYGNSS level 1 NBRCS for the period 18 March 2017 to 30 September 2017. To perform the analysis of wind speed under different precipitation conditions we use the Version 2.0 CYGNSS Level 3 gridded wind product [6] over the same time period. Precipitation information is obtained from the Version 4 final research run GPM IMERG gridded data. The CYGNSS level 3 product has a spatial resolution of (0.2x0.2) degree and a temporal resolution of 1hr. The GPM precipitation data is averaged over space and time to match up with the Level 3 CYGNSS wind data.

We use this matched up data to observe how CYGNSS winds vary under different precipitation conditions. Fig.1 shows how the global probability density function (PDF) of CYGNSS winds varies under low and high precipitation conditions. The precipitation information is obtained from the GPM IMERG Version 05 Final Run data product with a latency period of 2.5 months. The wind PDF is generated using the Level 3 CYGNSS wind product with the precipitation filter based on IMERG product matched to the resolution of CYGNSS Level 3 spatial and temporal resolution.

Here, precipitation less than 5mm/hr is considered low and greater than 10mm/hr is considered as high. We observe that the tail of the PDF is broader for high precipitation conditions. This can be attributed to a combination of the following reasons; 1) The downbursts cause high horizontal wind shear, 2) Attenuation of transmitted signal power due to heavy precipitation, 3) Drop in observed NBRCS due to rain induced surface roughening. In this work, we attempt to isolate these attributions by correcting for propagation losses and rain induced surface roughening due to heavy precipitation so that the effect of wind shear alone can be observed.

3. RAIN ATTENUATION CALIBRATION

In most situations, the earth's atmosphere is nearly transparent at the GPS L1 frequency. However, under heavy precipitation conditions the wind retrieval from the radar cross-section can be significantly affected. There is a twofold effect of rain on the observed radar cross-section. One is absorption by rain of electromagnetic energy along the propagation path of the signal. Second is increased sea-surface roughness caused by the rain, thereby further decreasing the observed NBRCS. In this section we model the effect of these two conditions and correct for the same in the CYGNSS measurements.

Let L_a represent the transmissivity accounting for losses due to absorption along the propagation path from the transmitter to the surface, resulting in a reduction in the received power.

$$L_a = \exp(-\tau_P) \quad (2)$$

$$\tau_P = \int_0^{Z_L \sec(\theta)} \alpha_P(z)\, dz \quad (3)$$

$$\alpha_P = \alpha_1(f) R^{b(f)} \quad (4)$$

The optical depth τ_P is evaluated from the surface up to the freezing level Z_L. θ is the incidence angle at the specular point and $\sec(\theta)$ accounts for the slant path of propagation. Over the tropics, the average height of the freezing level is approximately ~ 4800 ± 300 m [7]. The model for α_P, based on regression analysis from [8], is given by

$$\alpha_1(f) = 6.39 * 10^{-5} f^{2.03} \quad (5)$$

$$b(f) = 0.851 f^{0.158} \quad (6)$$

where f is the frequency in units of GHz, R is the rain rate in mm/hr, $\alpha_1(f)$ is the specific attenuation for a rain rate of 1mm/hr and $b(f)$ is an empirical constant. These expressions are considered valid for frequencies less than 2.9 GHz. To account for the variation in NBRCS due to increased surface roughness caused by downpour of rain, let us denote the perturbation in NBRCS due to downpour as $\delta\sigma_0^r(R)$. The surface roughness due to downpour is a superposition of rain induced surface features onto the capillary waves generated

due to the wind. In the bistatic configuration this superposition is going to reduce the observed NBRCS.

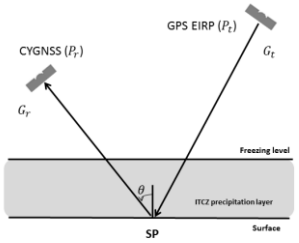

Fig. 2. Path of transmitted GPS signal through the heavy precipitation region.

$$\sigma_0^{obs} = \sigma_0 - \delta\sigma_0^r(R) \tag{7}$$

where $\delta\sigma_0^r$ is assumed to be a function of rain rate, R. A $\delta\sigma_0^r(R)$ model is developed empirically as follows. As the first step, under rain free condition, for a narrow range of wind speeds the NBRCS is calculated using the radar range equation given by Eq.1. Next, the NBRCS is calculated for a given precipitation condition R_r for the same range of wind speed using a modified forward model which accounts for the propagation loss, as described by

$$P_G(\tau, f) = T_i^2 \frac{P_T \lambda^2}{(4\Pi)^3} \mathbf{L_a^2} \iint \frac{G_T(\vec{\rho}) G_R(\vec{\rho}) F(\vec{\rho}) \Lambda^2(\tau, \vec{\rho}) |S(f, \vec{\rho})|^2 \boldsymbol{\sigma_0^{obs}}(\vec{\rho})}{R_0^2(\vec{\rho}) R^2(\vec{\rho})} d^2\rho \tag{8}$$

$$\sigma_0^{obs}|_R = \frac{P_G (4\pi)^3 R_0^2 R^2}{P_T \lambda^2 G_T G_R} \frac{\mathbf{1}}{\boldsymbol{L_a^2}} \tag{9}$$

An empirical model can then be derived according to

$$\delta\sigma_0^r|_R = <\sigma_0> - <\sigma_0^{obs}|_R> \tag{10}$$

where the expectation is performed over a large population of measurements [you need to specify in some detail what the population is; e.g. what time period, what locations, what PO.DAAC data version number] . This model is then used to correct the CYGNSS NBRCS measurements for surface roughening by the rain and the rain generated wind effects.

$$\widetilde{\sigma_0} = \sigma_0^{obs} + \delta\sigma_0^r(R) \tag{11}$$

GPM IMERG provides precipitation information with a spatial resolution of (0.1 x 0.1) deg and a temporal resolution of 30 mins. The height of the precipitation column is assumed to be a mean freezing level of 4800m. Fig.2 shows the region where the path loss due to precipitation will occur for a GPS-CYGNSS position.

In this work we plan to assimilate all DDM measurements of CYGNSS over different precipitation ranges obtained from GPM IMERG to obtain a model for rain induced surface roughening at GPS L1 frequency. The propagation loss and the developed model together are applied to the measured NBRCS to correct for the effect of precipitation on CYGNSS measurements.

4. MODEL FOR RAIN INDUCED SURFACE ROUGHENING AND INCREASE IN SURFACE WIND DUE TO RAIN

The rain induced surface roughening and the increase in surface wind associated with the presence of rain are modelled as the difference of the expectation of NBRCS distribution at no precipitation condition and expectation of NBRCS distribution at different precipitation conditions. Fig.3 shows the ideal NBRCS distribution when there is no precipitation.

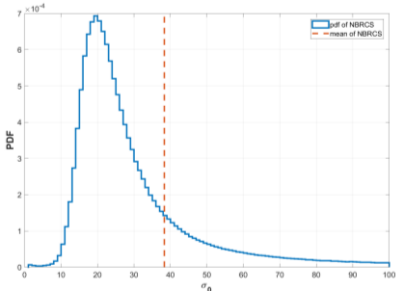

Fig. 3. PDF of NBRCS under no precipitation. The mean value is 38.352 (in numeric)

The sample population for different rain rates are developed by filtering the CYGNSS measurements based on GPM IMERG rain rates. The measurements are further filtered for the gain of CYGNSS receive antenna greater than 5dB to obtain good quality measurements. Fig.4 shows the sample population of CYGNSS specular point measurements at different rain rate conditions used in the model.

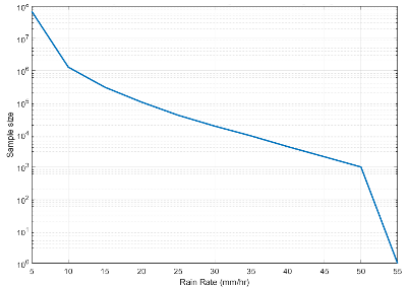

Fig. 4. CYGNSS sample density for different rain rates

To maintain quality of estimation we develop the model only up to 40 mm/hr as the number of samples is less than 10,000 for higher rain rates. The model developed is of the form:

$$\delta\sigma_0^r = a * R^b + c \tag{12}$$

Where a, b and c are tuning parameters and the model developed is shown in Fig. 5.

It is interesting to observe from Fig.5 that the dependence of roughening and increased wind on rain rate weakens above 10 mm/hr of rain. This model has an RMSE of 0.3072 and is used in calibrating the CYGNSS NBRCS for effect of precipitation. To the test the performance of the model, the CYGNSS measurements are assimilated for a rain rate of greater than 15 mm/hr and the developed corrections are applied.

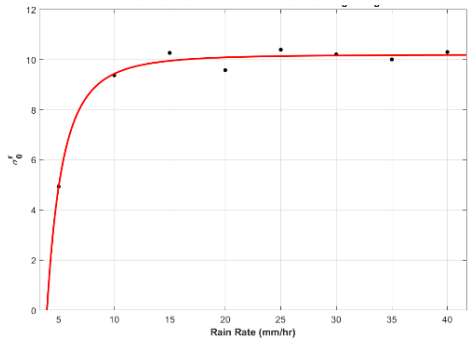

Fig. 5. Empirical model for rain induced surface roughness

Fig.6 shows the effect of calibration. Note that the error in the mean of the distribution drops considerably after the correction and the dominating factor for the improvement is the rain induced surface roughening correction when compared to propagation loss correction. It should be noted that this model folds into it the effect of additional wind actually generated due to rain which might be a contributing (and possibly the dominant) factor for this significant change in NBRCS after the correction. The mean value of the distribution before correction is 27.4906, after the propagation loss correction is 28.1030 and after including the effects of rain induced surface roughening is 37.9496. The expected value of the distribution is much closer to the actual expected value shown in Fig.3.

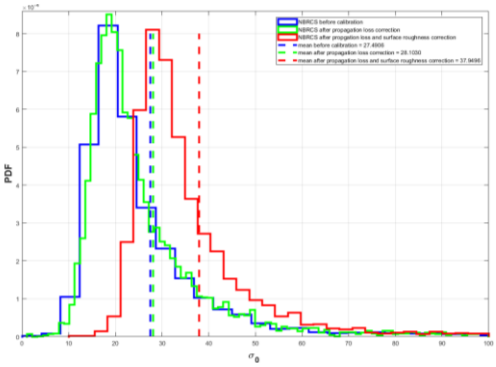

Fig. 6. PDF of CYGNSS measurements before and after correction for a rain rate > 15 mm/hr.

5. CONCLUSION

In this work, we have applied a rain correction to CYGNSS DDM measurements to account for its sensitivity to surface winds under high precipitation conditions and to observe the strong horizontal wind shear produced in the tropical rain bands of the ITCZ. Future work in this direction will involve careful study of the impact of relative height of the freezing level with respect to the horizontal resolution [9] and the related edge effects in the correction terms for CYGNSS measurements.

6. REFERENCES

[1] C S., Ruf, P Chang, M P., Clarizia, S Gleason, Z Jelenak, J Murray, M Morris, S Musko, D Posselt, D Provost, et al., "CYGNSS handbook," *Ann Arbor, MI, USA: Michigan Publishing*, 2016.

[2] Nereida Rodriguez-Alvarez, Dennis M., Akos, Valery U., Zavorotny, Jeffreyand Camps Adriano Smith, A., and Christopher W Fairall, "Airborne GNSS-R wind retrievals using delay–doppler maps," *IEEE Transactions on Geoscience and Remote Sensing*, vol. 51(1), pp. 626–641, 2013.

[3] M P., Clarizia, C P., Gommenginger, S Gleason, M A., Srokosz, C Galdi, and M Di Bisceglie, "Analysis of GNSS-R delay-doppler maps from the UK-DMC satellite over the ocean," *Geophysical Research Letters*, vol. 36(2), 2009.

[4] Scott Gleason, Christopher S., Ruf, Maria P., Clarizia, and Andrew J., O'Brien, "Calibration and unwrapping of the normalized scattering cross section for the cyclone global navigation satellite system," *IEEE Transactions on Geoscience and Remote Sensing*, vol. 54(5), pp. 2495– 2509, 2016.

[5] Valery U Zavorotny and Alexander G Voronovich, "Scattering of GPS signals from the ocean with wind remote sensing application," *IEEE Transactions on Geoscience and Remote Sensing*, vol. 38, no. 2, pp. 951–964, 2000.

[6] Christopher S., Ruf , "Algorithm Theoretical Basis Document Level 3 Gridded Wind Speed," *ClaSp, Univ. of Michigan, UM Doc. No. 148-0319.*

[7] Harris Jr, Gettys N., Kenneth P. Bowman, and Dong-Bin Shin. "Comparison of freezing-level altitudes from the NCEP reanalysis with TRMM precipitation radar brightband data." *Journal of Climate* vol. 13(23), pp. 4137-4148, 2000.

[8] Ulaby, Fawwaz Tayssir, et al. "Microwave radar and radiometric remote sensing". Vol. 4. No. 5. Ann Arbor: University of Michigan Press, 2014.

[9] Morris, M. and Ruf, C.S., A coupled-pixel model (CPM) atmospheric retrieval algorithm for high-resolution imagers. *Journal of Atmospheric and Oceanic Technology*, Vol. 32, no. 10, pp.1866-1879, 2015.